Journal of proteome research

pubs.acs.org/jpr

Article

Spontaneous Glycan Reattachment Following N-Glycanase Treatment of Influenza and HIV Vaccine Antigens

Celina L. Keating,[▽] Eric Kuhn,[▽] Julia Bals,[▽] Alexandra R. Cocco,[▽] Ashraf S. Yousif,[▽] Colette Matysiak, Maya Sangesland, Larance Ronsard, Matthew Smoot, Thalia Bracamonte Moreno, Vintus Okonkwo, Ian Setliff, Ivelin Georgiev, Alejandro B. Balazs, Steven A. Carr,* and Daniel Lingwood*

Cite This: *J. Proteome Res.* 2020, 19, 733−743

Read Online

ACCESS | Metrics & More | Article Recommendations | Supporting Information

ABSTRACT: In cells, asparagine/N-linked glycans are added to glycoproteins cotranslationally, in an attachment process that supports proper folding of the nascent polypeptide. We found that following pruning of *N*-glycan by the amidase PNGase F, the principal influenza vaccine antigen and major viral spike protein hemagglutinin (HA) spontaneously reattached *N*-glycan to its de-N-glycosylated positions when the amidase was removed from solution. This reaction, which we term N-glycanation, was confirmed by site-specific analysis of HA glycoforms by mass spectrometry prior to PNGase F exposure, during exposure to PNGase F, and after amidase removal. Iterative rounds of de-N-glycosylation followed by N-glycanation could be repeated at least three times and were observed for other viral glycoproteins/vaccine antigens, including the envelope glycoprotein (Env) from HIV. Covalent *N*-glycan reattachment was nonenzymatic as it occurred in the presence of metal ions that inhibit PNGase F activity. Rather, N-glycanation relied on a noncovalent assembly between protein and glycan, formed in the presence of the amidase, where linearization of the glycoprotein prevented this retention and subsequent N-glycanation. This reaction suggests that under certain experimental conditions, some glycoproteins can organize self-glycan addition, highlighting a remarkable self-assembly principle that may prove useful for re-engineering therapeutic glycoproteins such as influenza HA or HIV Env, where glycan sequence and structure can markedly affect bioactivity and vaccine efficacy.

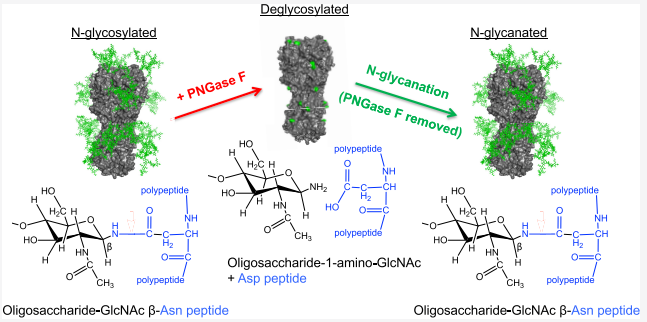

KEYWORDS: *deglycosylation, amidase, N-glycanation, spontaneous, N-glycan, reattachment, NXS/T sequon, glycoprotein, test tube, self-organizing*

Downloaded via HARVARD UNIV on March 7, 2020 at 17:12:44 (UTC).
See https://pubs.acs.org/sharingguidelines for options on how to legitimately share published articles.

INTRODUCTION

Asparagine (Asn) N-glycosylation is a universally conserved post-translational modification, occurring in all three domains of life, eukaryotes, bacteria, and archaea.[1−3] In metazoans and many eukaryotes, N-glycans are formed as β-linkages between acetylglucosamine (GlcNAc) and asparaginyl residues within NXS/T sequons.[2−4] Energetically, the attachment process is largely driven by enzymatic cleavage of a high-energy GlcNAc−phosphate bond within an oligosaccharide donor molecule.[5−7] However, glycan attachment is also cotranslational, and thermodynamic modeling predicts coupling between folding of the nascent polypeptide chain and *N*-glycan addition.[8−10] In this study, we uncovered a previously unrecognized reaction that experimentally highlights a link between protein structure and the formation of the GlcNAc−β-Asn linkages. After treating the principal vaccine influenza vaccine antigen and major viral spike glycoprotein hemagglutinin (HA) with PNGase F, an amidase that catalyzes the cleavage of the N-linked bond converting Asn to Asp,[11−14] we found that the de-N-glycosylated HA spontaneously transitioned back to its native N-glycanated state when PNGase F was removed from solution. Transitioning between these two states was nonenzymatic and could be cycled repeatedly. During this process, reattachment occurred at the same PNGase F-deaminated positions and was preceded by noncovalent retention of the cleaved glycan. If HA was linearized to destroy protein conformation, then both retention and subsequent reattachment of *N*-glycan were prevented. Glycan reattachment was also observed for HIV envelope glycoprotein (Env), an unrelated viral glycoprotein/vaccine antigen.[15,16] This new reaction, which we term N-glycanation, suggests that under certain experimental conditions, aspects of three-dimensional protein structure may serve to modulate and organize *N*-glycan addition. Moreover, N-glycanation points out a potential means of re-engineering glycan sequences of

Received: September 11, 2019
Published: January 8, 2020

© 2020 American Chemical Society

https://dx.doi.org/10.1021/acs.jproteome.9b00620
J. Proteome Res. 2020, 19, 733−743

therapeutic glycoproteins in the test tube, such as influenza HA or HIV Env, where glycan structure and sequence regulate bioactivity and vaccine efficacy.[17−21]

MATERIALS AND METHODS

Recombinant Proteins

All proteins were expressed in 293F cells using pVRC8400, a plasmid containing the CMV IE enhancer/promoter, HTLV-1 R region and splice donor site, and the CMV IE splice acceptor site upstream of the open reading frame:[22] the soluble trimeric configurations of the trimerized HA ectodomains from A/New Caledonia/20/1999 (H1N1); A/Indonesia/5/2005 (H5N1); and A/Wisconsin/67/2005 (H3N2) were expressed in 293F cells and purified using a combination of affinity and size exclusion chromatography as described previously.[22−24] In this study, we focused on the H1 HA trimer, referred throughout as HA trimer. The hemagglutinin trimers from H3N2 and H5N1 are denoted H3 and H5, respectively. To prevent aggregation of the trimers, they were cotransfected with influenza strain-matched neuraminidase (NA).[22] For experiments with trimers bearing terminal sialyl-oligosaccharide (SA), they were purified with the Y98F substitution that prevents SA binding but maintains the structural integrity of the binding site.[23,25] The gp120 core of HIV Env from clade B virus (strain HT593.1) was expressed and purified on a 17b antibody column, as described previously.[15,16] Fetal bovine fetuin was obtained from Sigma-Aldrich (Cat #F2379, Sigma-Aldrich).

Spontaneous Reformation of PNGase F Substrate by Influenza HA

Purified influenza H1 HA trimer was first de-N-glycosylated under nondenaturing conditions using commercial PNGase F tagged with a chitin-binding domain (CBD) (Remove-iT PNGase F, Cat #P0706S, New England BioLabs) (=CBD-PNGase F) according to the manufacturer's instructions (0.72 mg/mL HA, 40 000 units/mL CBD-PNGase F, 50 mM Na_3PO_4, pH 7.5; 24 h incubation at 37 °C). Chitin magnetic beads (Cat #E8036S, New England BioLabs) equilibrated CBD binding buffer (500 mM NaCl, 20 mM Tris−HCI, 1 mM EDTA, pH 8) were incubated with the deglycosylation reaction (1 h at 4 °C, RotoFlex Plus Tube Rotator, Argos Technologies) and then applied to deplete CBD-PNGase from solution via separation on a magnetic column (NEB cat. S1509), as per the manufacturer's instructions. To ensure separation of HA and CBD-PNGase F, the reaction was further separated on a Superdex 200 10/300 size exclusion column (SEC) using an automated FPLC system (Acta pure 2L, GE). Each step (input, de-N-glycosylation, post-PNGase F removal) was visualized by SDS PAGE where gels were stained with GelCode Blue (Thermo Scientific, MA). To visualize protein glycan, the gels were also stained using the periodate-acid Schiff (PAS) reagent method using a commercially available glycoprotein staining kit (Pierce Glycoprotein Staining Kit, ThermoFisher). To confirm spontaneous reformation of PNGase F substrate, cycles of CBD-PNGase F exposure and removal were performed on the same HA preparation using the same conditions.

The above experiments were performed with a recombinant HA trimer in which the terminal sialyl-oligosaccharide (SA) of its glycan chains was cleaved by coexpression with neuraminidase, a procedure that prevents in-solution aggregation of the trimers due to HA lectin activity for SA, the receptor for influenza virus.[22,25] To perform the procedure with terminal SA present, we generated Y98F HA, a mutation that prevents SA binding but maintains the integrity of the HA receptor binding site (RBS).[25] In this case, we monitored HA deglycosylation and then PNGase F substrate reformation by Western blotting with SNA-lectin, as described previously.[26,27] Briefly, SDS PAGE was performed as above, and the proteins were transferred to nitrocellulose (Trans-Blot SD Semi-Dry Transfer Cell, BioRad), and the blots were then blocked in an Odyssey blocking buffer (cat. 927-40100, LI-COR). The blots were then incubated with biotinylated SNA (cat. B-1305, Vector Labs; 2 μg/mL in blocking buffer), washed 3× in PBS, and then incubated with streptavidin-conjugated IRDye800CW (cat. 926-32230, LI-COR; 1/5000 in blocking buffer). The blots were then washed 3× with PBS and developed on an Odyssey CLx Imaging System (LI-COR).

Proteome Analysis of Hemagglutinin A by LC−MS

Gel bands for HA at each stage (pretreated, CBD-PNGase F-treated, and after amidase removal; for the latter, we ensured separation from CBD-PNGase F, using chitin affinity beads followed by SEC) were excised, cut into smaller pieces, and transferred into 1.5 mL tubes. Gel bands were destained with 500 μL of 50% acetonitrile/50% of 100 mM ammonium bicarbonate pH 8.1, mixed at 850 RPM for 10 min at room temperature (RT). Buffer was removed using a gel loading pipet tip, and the process was repeated until no further stain was removed. Bands were washed and hydrated with 100 mM ammonium bicarbonate pH 8.1 for 5 min, mixed at 850 RPM at RT, and subsequently dehydrated with 100% acetonitrile for 5 min at 850 RPM at RT. Bands were reduced with 10 mM DTT 100 mM ammonium bicarbonate pH 8.1, incubated 30 min, mixing at 1000 RPM at 37 °C, dehydrated with 100% acetonitrile (5 min, 1000 RPM, RT), and then alkylated with 30 mM iodoacetamide 100 mM ammonium bicarbonate 30 min at 1000 RPM at RT in the dark. Prior to trypsin digestion, gel bands were dehydrated with 100% acetonitrile 5 min at 1000 RPM at 37 °C. Trypsin was diluted to 14 ng/μL in 100 mM ammonium bicarbonate, added to each gel band in sufficient volume to cover each gel piece (∼50 μL), and incubated overnight at 850 RPM and 37 °C (∼16 h). On the next day, a second volume of a 14 ng/μL trypsin solution was added to cover the bands (∼50 μL) and incubated 1 h at 850 RPM and 37 °C. After collecting the supernatant, three subsequent extractions with 50% acetonitrile/50% of 100 mM ammonium bicarbonate were performed to extract the peptide bands. For each extraction step, the solvent was incubated for 10 min at 850 RPM at RT. The peptide bands were further treated with 100% acetonitrile until completely dehydrated. All of the acetonitrile supernatants were added to the peptide extracts, frozen, and dried by vacuum centrifugation. The dried peptide extracts were resuspended in 40 μL of 3% acetonitrile/0.1% formic acid and desalted using a 3 punch Empore C18 packed StageTip. StageTips were washed and equilibrated with 50 μL of 90% acetonitrile/0.1% TFA followed by 50 μL of 0.1% TFA prior to use. Samples were loaded onto StageTips, washed with 2 × 50 μL of 0.1% TFA, and then eluted with 2 × 30 μL of 40% acetonitrile/0.1%TFA. Desalted peptide extracts were transferred to HPLC vials, frozen, dried using vacuum centrifugation, and stored at −80 °C until LC−MS/MS analysis.

LC−MS/MS analysis

Samples were resuspended in 10 μL of 3% acetonitrile/5% acetic acid, mixed and centrifuged briefly (∼30 s), and analyzed on a QExactive mass spectrometer (Thermo) equipped with a Proxeon Easy-nLC 1200 and a custom-built nanospray source

https://dx.doi.org/10.1021/acs.jproteome.9b00620
J. Proteome Res. 2020, 19, 733−743

(James A. Hill Instrument Services). MS acquisition was performed using Xcalibur software version 3.0.63. Samples were injected (40% of sample) onto a 75 μm ID PicoFrit column (New Objective) manually packed to 20 cm with Reprosil-Pur C18 AQ 1.9 μm media (Dr. Maisch) and heated to 50 °C. MS source conditions were set as follows: spray voltage 2000, capillary temperature 250, S-lens RF level 50. A single Orbitrap MS scan from 300 to 1800 m/z at a resolution of 70 000 with AGC set at 3e6 was followed by up to 12 MS/MS scans at a resolution of 17 500 with AGC set at 5e4. MS/MS spectra were collected with a normalized collision energy of 25 and an isolation width of 2.5 amu. Dynamic exclusion was set to 20 s, and the peptide match was set to preferred. Mobile phases consisted of 3% acetonitrile/0.1% formic acid as solvent A, and 90% acetonitrile/0.1% formic acid as solvent B. Flow rate was set to 200 nL/min throughout the gradient, 2−6% B in 1 min, 6−30% B in 84 min, 30−60% B in 9 min, and 60−90% B in 1 min with a hold at 90% B for 5 min.

MS data were searched against a UniProt database containing human reference proteome sequences downloaded from the UniProt web site on October 17, 2014, with redundant sequences removed using Byonic software v2.16.11 (Protein Metrics). A set of common laboratory contaminant proteins (150 sequences) and the expressed hemagglutinin A H1 sequence were appended to this database. Search parameters: cleavage residues RK, fully specific termini, 1 missed cleavage, QTOF/HCD fragmentation, 20 ppm precursor, and fragment tolerance. Fixed modifications: carbamidomethylation at cysteine. Variable modifications: N-term Gln → pyroGlu, N-term Glu → pyroGlu, ammonia-loss, deamidation, oxidation of methionine and tryptophan, dethiomethyl methionine, decarbamidomethyl cysteine, C-term sodiation, and 38 N-linked glycan common biantennary modifications. Spectra were further searched against a decoy database, and the database match threshold was set to 1% FDR at the protein level. The specific sugar units are based on the known biosynthesis of N-linked sugars as the MS and MS/MS alone do not distinguish/identify the specific HexNAc, hexose, deoxyhexose, etc. that are present.

Precursor masses of identified unmodified and modified peptides, including all identified glycoforms, were extracted using XCalibur Qualbrowser software (Thermo) 3.0.63. Peak height intensity for each precursor m/z in the extracted ion chromatogram (XIC) was tabulated and used to estimate the relative peptide abundance in each sample. The intensity values were normalized for the amount of HA in each lane using a nonglycosylated HA peptide, IDGSGYIPEAPR. To estimate glycan reoccupancy, the MS response for each detected glycoform was divided by the normalized MS response for the corresponding peptide in the pretreatment samples. The in-gel digestion LC−MS workflow is described in Figure S1.

To evaluate glycan reoccupancy, the following calculations were made. The HA gel bands were designated as band 1 (pretreatment), band 2 (PNGase F-treated), and band 3 (after amidase removal) (Figure S1). The normalized intensity MS signal for each glycosylated form of the peptide (e.g., [+1445], [+1607], [+1769], etc.) identified in band 2 (when detected or signal given as 0) was divided by the corresponding MS signal in band 1 (eq 1). The same calculation was performed for band 3 (eq 2). This was calculated for each HA peptide identified using Byonic that contained a consensus N-linked glycosylation consensus motif (NXS/T)

$$\frac{(\text{band2})N[+1445]\text{GTYDYPK}}{(\text{band1})N[+1445]\text{GTYDYPK}} \quad (1)$$

$$\frac{(\text{band3})N[+1445]\text{GTYDYPK}}{(\text{band1})N[+1445]\text{GTYDYPK}} \quad (2)$$

These resulting ratios demonstrate the loss and subsequent reattachment of glycans to each peptide as compared to those in band 1 or untreated HA. A complete work-through for this glycan analysis pipeline is presented in Figure S1.

Assaying for Noncovalent Glycan Complex Formation

De-N-glycosylation of HA was performed under nondenaturing conditions using commercially available PNGase F (no affinity tag) (Cat # P0705L, New England BioLabs) according to the manufacturer's instructions (0.72 mg/mL HA, 40 000 units/mL PNGase F, 50 mM Na_3PO_4, pH 7.5; 24 h incubation at 37 °C). We then separated the same reaction mixture by SDS PAGE or by blue native PAGE as previously described.[28] The gels were then stained with GelCode Blue to detect protein or the PAS reagent method to detect glycan, as described above. To ensure that the PAS signal could be precisely compared with the GelCode Blue signal, the GelCode blue stain was applied first and then removed (microwave 2 min), following which time the PAS staining for glycan was applied.

N-Glycanation during Size Exclusion Chromatography

To test if the noncovalently bound amidase-liberated carbohydrate reformed PNGase F substrate when physically separated from the amidase, the HA-PNGase F de-N-glycosylation reaction was immediately separated by SEC (no pre-in-solution depletion using affinity beads) using a Superdex 200 10/300 size exclusion column, which would separate free glycan from HA and also HA away from PNGase F. The separated HA was then separated by SDS PAGE and re-exposed to PNGase F. These products were then evaluated by SDS PAGE with GelCode Blue and PAS staining.

Conformational Requirements for N-Glycanation

To evaluate the contribution of conformational protein structure to noncovalent interactions with amidase-liberated glycan and the subsequent N-glycanation, we heat-denatured HA (100 °C for 30 min) and then deglycosylated with PNGase F. The substrates and products of the PNGase F deglycosylation reaction were first evaluated by native PAGE with GelCode Blue and PAS staining. The corresponding capacity for N-glycanation was evaluated by separating the denatured HA + PNGase F by SEC and monitoring the input and output HAs by SDS PAGE. To further explore this, we mixed HA trimer with heat-denatured HA, deglycosylated the protein mixture together, and then removed the PNGase F by SEC and analyzed the fractions by SDS PAGE.

N-Glycanation in the Presence of Mn^{2+}

Given that N-glycanation could also be achieved on the size exclusion column (Superdex 200 10/300), we applied SEC to assay for N-glycanation in the presence of 1 mM Mn^{2+}, where this metal ion concentration has been reported to inhibit the catalytic activity of PNGase F.[29] The purpose of this experiment was to rule out the enzymatic contribution of PNGase F to the glycan reattachment process. For this, we obtained a commercial PNGase F prep that did not contain metal ion chelators (Agilent, cat. GKE-5016B) and performed the 24 h deglycosylation procedure on HA (as described earlier) but

https://dx.doi.org/10.1021/acs.jproteome.9b00620
J. Proteome Res. 2020, 19, 733−743

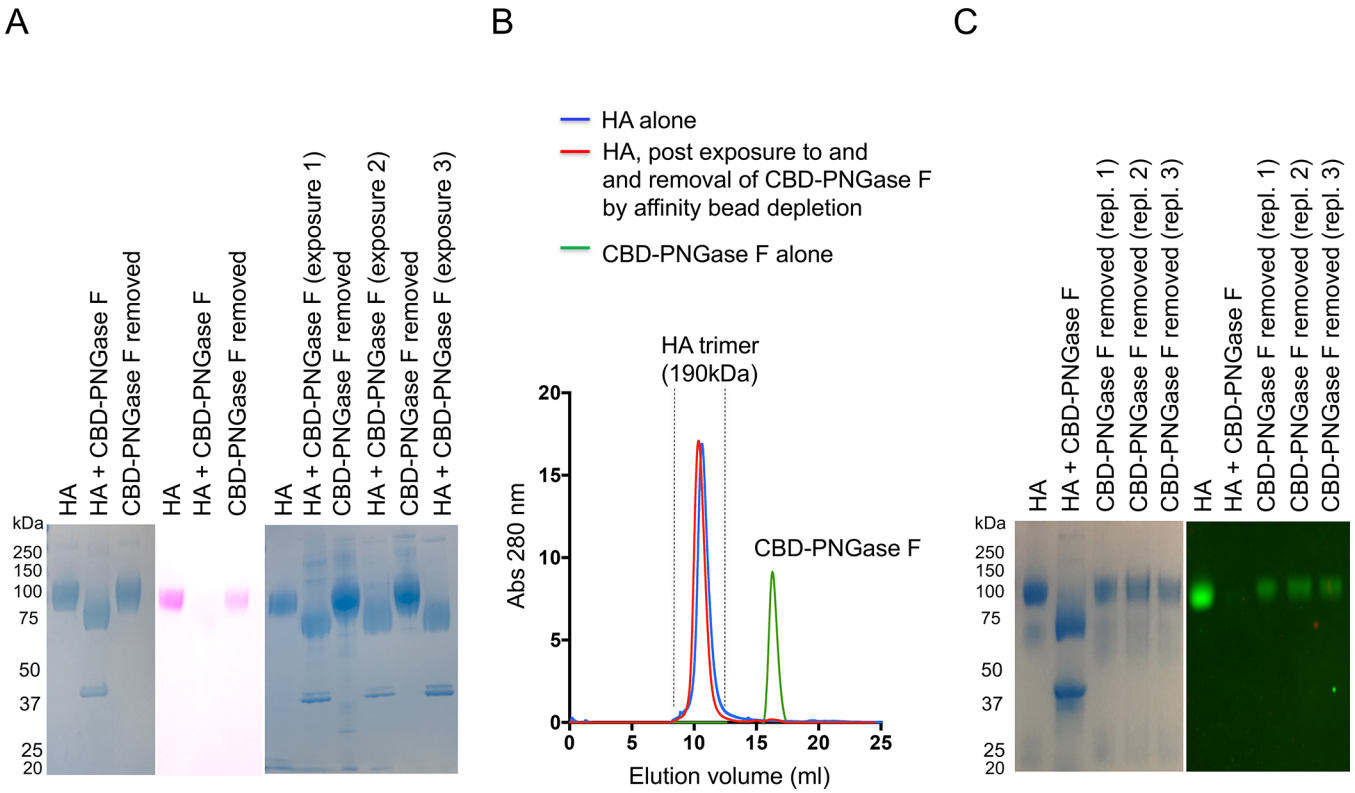

Figure 1. N-Glycanation as initially identified as the spontaneous reformation of amidase substrate following cleavage by PNGase F, a reaction that could be cycled indefinitely. (A) HA was de-N-glycosylated using chitin-binding domain (CBD)-PNGase F, which when removed by magnetic chitin protein beads was concomitant with recovery in HA's electrophoretic mobility (GelCode Blue staining), glycan stain (PAS) (pink), and reacquired sensitivity to CBD-PNGase F (three iterative cycles of de-N-glycosylation by amidase exposure + recovery after amidase removal are shown). (B) HA and "glycan-recovered HA" were also further separated by SEC (Superdex 200 10/300 column). (C) Recombinant HA was coexpressed with NA to cleave terminal SA to prevent aggregation in solution. To assess the reformation of amidase substrate when terminal SA was present, Y98F HA trimer was used (GelCode Blue stain and Western blot using SNA to detect SA).

now in 50 mM Tris, pH 8.0 $MnCl_2$. After confirming the inhibitory activity of Mn^{2+} (SDS PAGE with GelCode Blue stain), we repeated the HA deglycosylation by PNGase F within 50 mM Tris, pH 8.0, but in the absence of Mn^{+2}. This reaction was then separated into two samples: (1) control deglycosylated HA and (2) deglycosylated HA that was then adjusted to 1 mM $MnCl_2$. We then performed SEC where the FPLC system and column were pre-equilibrated with either 50 mM Tris, pH 8.0 (for control sample) or 50 mM Tris, 1 mM $MnCl_2$, pH 8.0 (for Mn^{2+}-adjusted sample). In both cases, we observed a single peak on the chromatogram corresponding to HA trimer, which was then collected and evaluated by SDS PAGE with GelCode Blue stain.

N-Glycanation in Other Viral Glycoproteins/Vaccine Antigens

We used the SEC protocol to assay for N-glycosylation by other viral surface glycoproteins including distantly related H3 and H5 influenza trimers and also the unrelated glycoprotein HIV Env. The glycoprotein fetal bovine fetuin was also evaluated in parallel. Following PNGase F glycosylation and amidase separation by SEC (Superdex 200 10/300), we analyzed the pre- and post-treated glycoproteins by SDS PAGE with GelCode Blue stain or PAS reagent method to detect glycan.

RESULTS

N-Glycanation As Initially Identified by SDS PAGE

HA is a trimeric protein, assembled from protomers of ~65 kDa, which also bear the added mass of N-glycosylation.[13,30] Protein N-glycans, including those of HA, have traditionally been analyzed following PNGase F de-N-glycosylation of denatured glycoprotein substrate.[11−14,30,31] We found that pruning HA with PNGase F under nondenaturing conditions resulted in a decrease in a molecular mass of ~30 kDa and loss of detection using a specific stain for glycans (Figure 1A). We then removed the amidase from solution with magnetic chitin beads (PNGase F was affinity-tagged with a chitin-binding domain = CBD-PNGase). Amidase removal by this method was completed in less than 2 h, and the input/output forms of HA were immediately evaluated by SDS PAGE. Following removal of the amidase, we observed that HA returned to native electrophoretic mobility, reacquired sensitivity to glycan staining by the periodate-acid Schiff (PAS) reagent, and reacquired sensitivity to CBD-PNGase F (Figure 1A). Indeed, the same HA substrate could be passed through multiple cycles of de-N-glycosylation followed by electrophoretic recovery (Figure 1A), indicating a highly repeatable process in which CBD-PNGase F substrate was first enzymatically cleaved and then reformed. To further ensure that CBD-PNGase F had been separated from HA by our magnetic beads, we fractionated the mixture by size column chromatography (SEC) under non-denaturing conditions using a Superdex 200 10/300 column,

https://dx.doi.org/10.1021/acs.jproteome.9b00620
J. Proteome Res. 2020, 19, 733−743

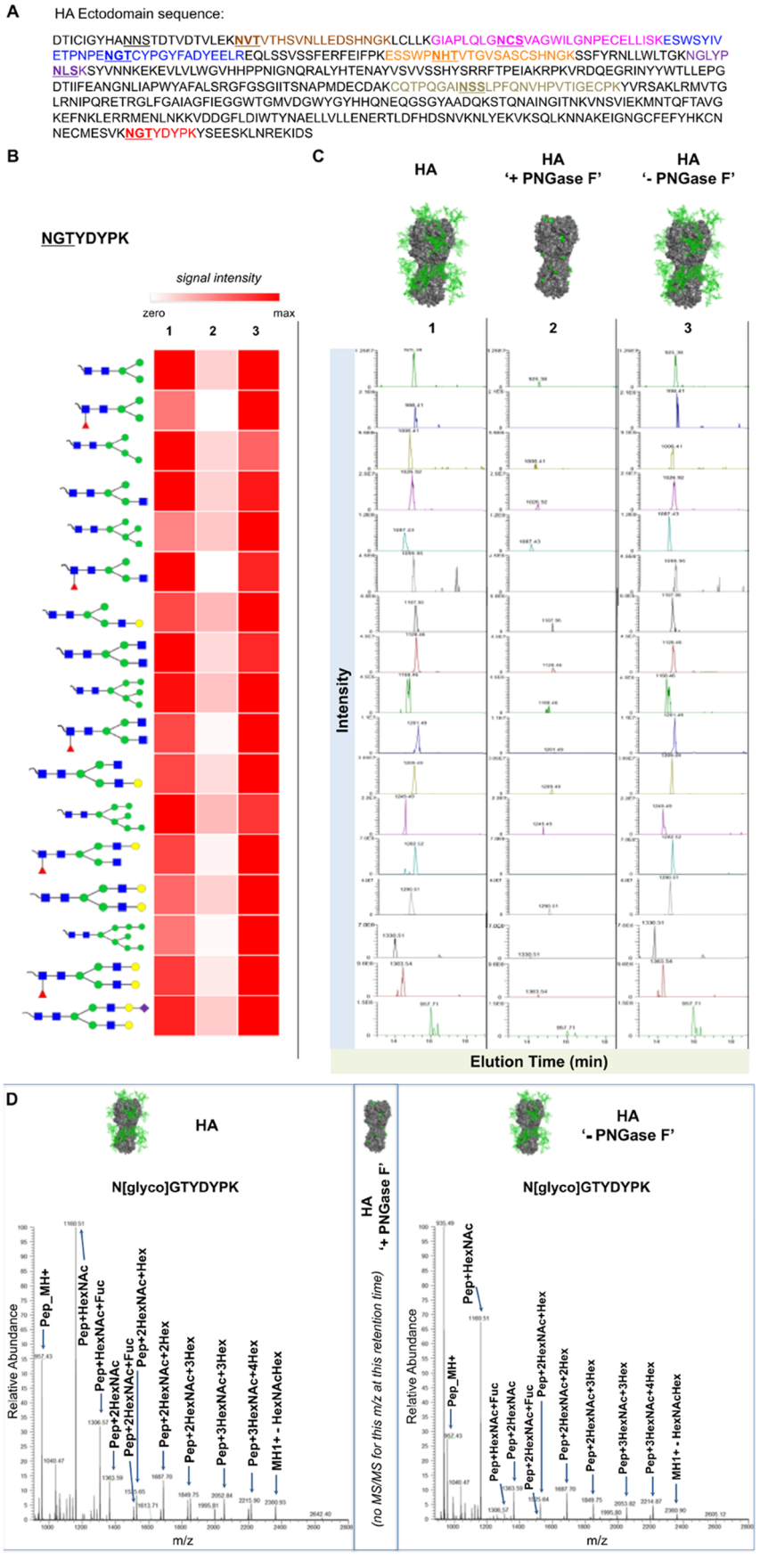

Figure 2. continued

https://dx.doi.org/10.1021/acs.jproteome.9b00620
J. Proteome Res. 2020, 19, 733−743

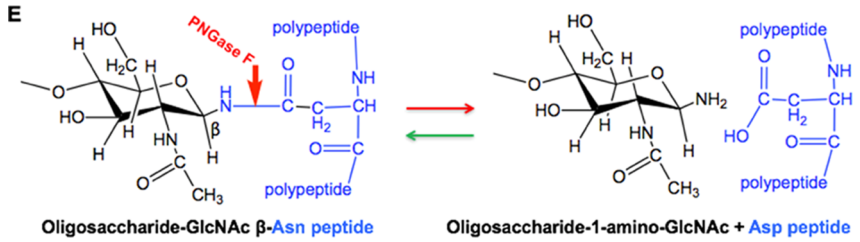

Figure 2. N-glycans reattach to the same former glycosylation-site peptides of HA and have similar carbohydrate compositions. (A) Amino acid sequence of HA, with potential N-linked glycosylation sites underlined. Bolded underlines indicate glycosites observed in glycopeptides and as-deamidated peptides following digestion with PNGase F. In-gel trypsin digests of HA isolated at each stage of the glycanation reaction separated by SDS PAGE (before, post-de-N-glycosylation, and post-PNGase F removal) were analyzed by LC−MS/MS. (B) Relative MS intensity heat map of the 17 detected glycoforms of HA peptide NGTYDYPK identified [before (1) de-N-glycosylation in the presence of PNGase F (2) and post-PNGase F removal (3)]. Relative intensities were adjusted for the total amount of HA in the sample. (C) Extracted ion chromatograms (XICs) of the precursor masses for each of the corresponding glycan structures shown in (A). The mass spectra corresponding to the data shown in panels B and C are shown in Supporting Figure 3, and results for the other six glycopeptides are presented in Supporting Figures 4−9. (D) MS/MS spectra of glycopeptide N[glyco] GTYDYPK before PNGase F treatment (left) and after PNGase F and glycan reattachment. For both conditions, the site of attachment of the glycan ([HexNAc(4)Hex(5)Fuc(1)], mass of adduct = 1768.6, MW glycopeptide = 2725.1) was confirmed by the MS/MS spectra of the doubly charged precursor of the $(M + 2H)^{2+}$ of the glycopeptide = 1363.543. As indicated in the center of (D), no MS/MS was obtained for this m/z at or near this retention time during exposure to PNGase F. (E) Proposed reaction scheme for glycan reattachment by reverse hydrolysis.

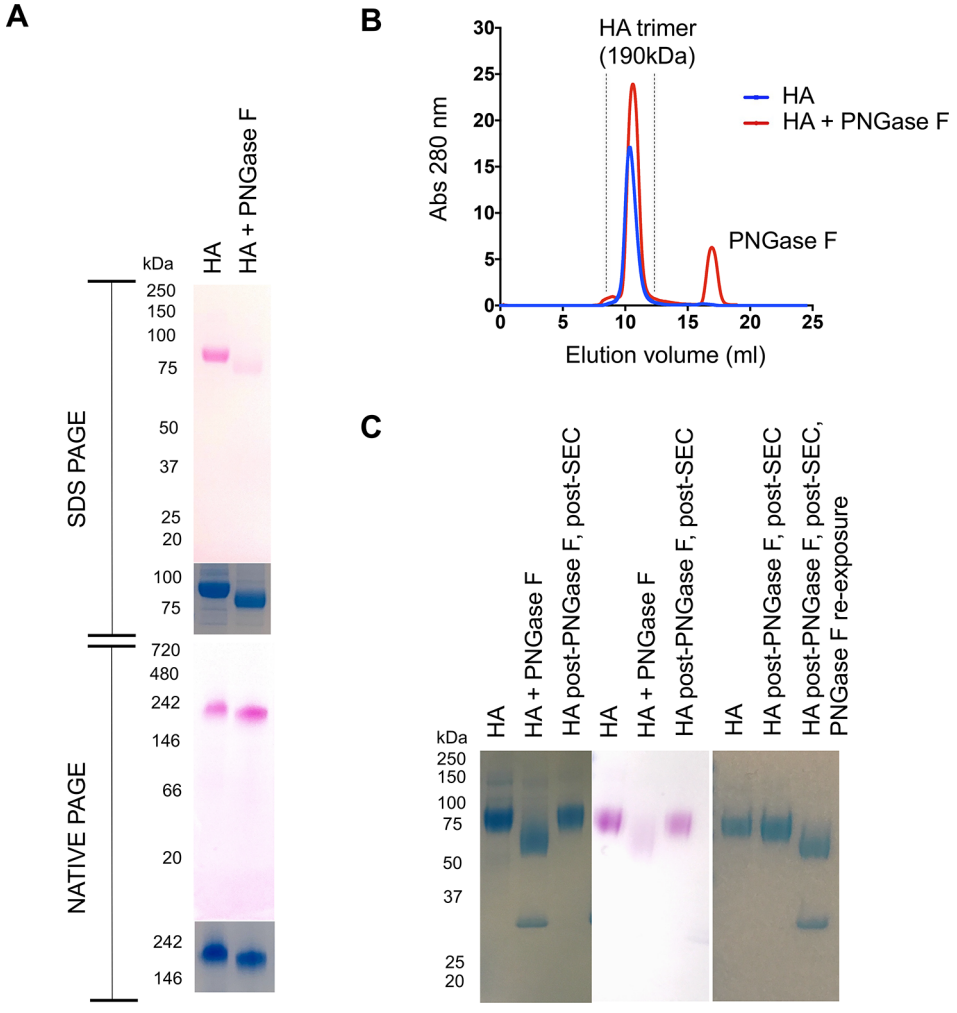

Figure 3. N-glycanation is preceded by noncovalent retention of cleaved *N*-glycan. (A) HA was de-N-glycosylated by PNGase F, and the mixture was separated by SDS PAGE or native PAGE without prior removal of PNGase F. The gels were stained with PAS to mark glycan (pink) and also GelCode Blue for protein. (B) To further define noncovalent retention of *N*-glycan following cleavage by PNGase F, the HA + PNGase F de-N-glycosylation reaction was immediately separated by SEC (Superdex 200 10/300 column; in this case, no chitin beads were used to pre-remove the amidase from solution). (C) HA product of this SEC was then analyzed for N-glycanation by SDS PAGE (GelCode blue for protein, PAS to mark glycan, and re-exposure to PNGase F to mark reformation of amidase substrate).

https://dx.doi.org/10.1021/acs.jproteome.9b00620
J. Proteome Res. 2020, 19, 733−743

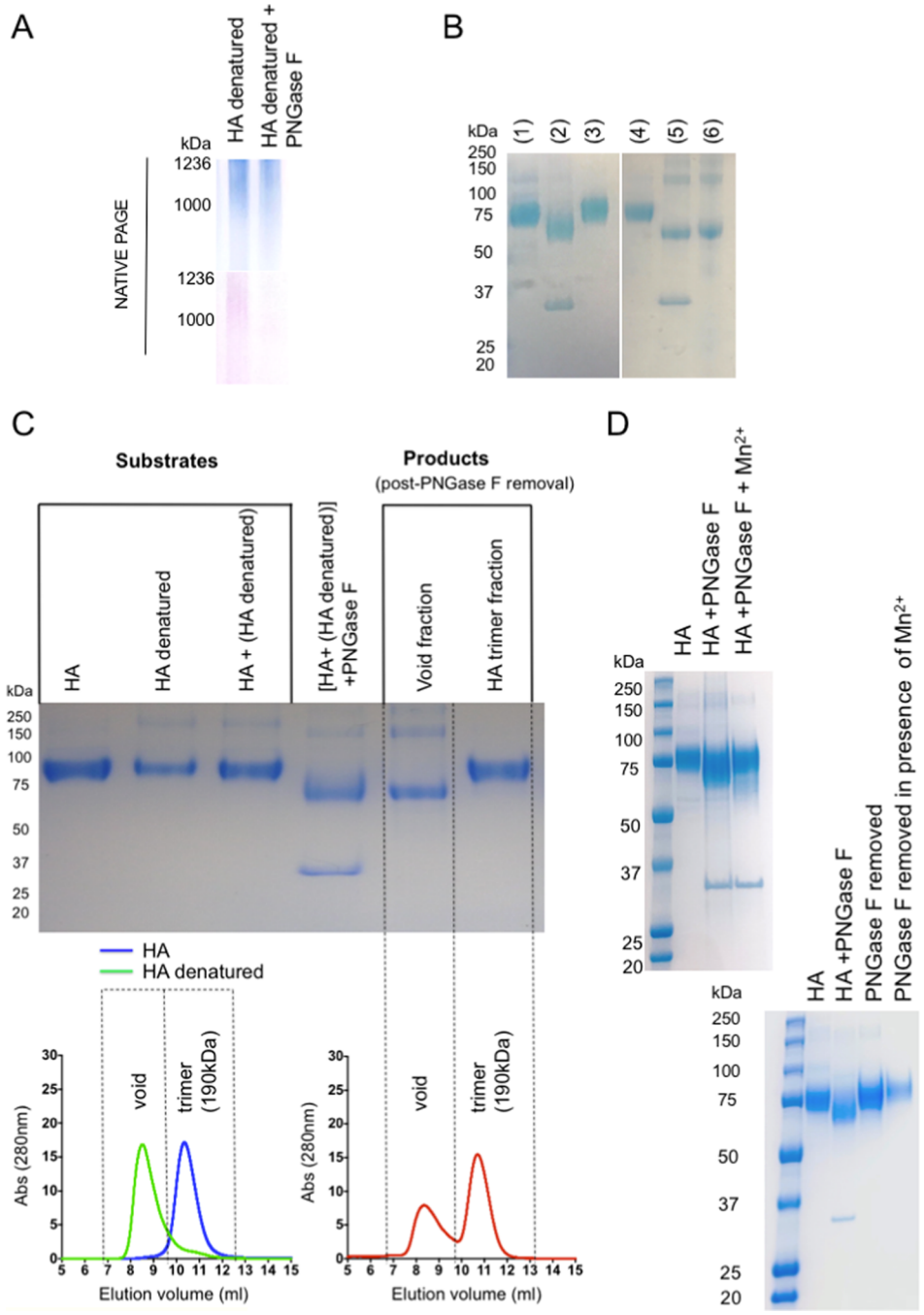

Figure 4. Nonenzymatic but conformational requirement for glycan retention and N-glycanation. (A) If HA was denatured (100 °C for 30 min), it no longer retained glycan in the presence of PNGase F, as marked by native PAGE followed by GelCode Blue stain for protein (blue) and PAS stain for glycan (pink). (B) Heat-denatured HA also no longer served as substrate for N-glycanation, as evaluated by de-N-glycosylation by PNGase F followed by SEC and SDS PAGE and GelCode Blue staining. Lanes 1−3 are for a control N-glycanation reaction (1 = HA; 2 = HA + PNGase F; 3 = HA recovered post PNGase F treatment and post separation by SEC). Lanes 4−6 denote the same reaction except with heat-denatured HA as substrate (4 = HA; 5 = HA + PNGase F; 6 = HA recovered post PNGase F treatment and post separation by SEC). (C) Denatured HA was mixed with folded trimeric HA, and the mixture was de-N-glycosylated by PNGase F and the capacity for N-glycanation was evaluated by SDS PAGE (GelCode Blue stain) before and after separation by SEC (Superdex 200 10/300 column). Both HA and denatured HA could be separated by SEC. Both HA forms also underwent de-N-glycosylation together (shift in MW in the SDS PAGE readout), but only denatured HA fraction remained de-N-glycosylated after chromatographic separation from the amidase. HA recovered from the trimeric elution volume on SEC had now reacquired the glycan. (D) Upper gel: we confirm Mn^{2+} as an inhibitor of deglycosylation activity by PNGase F. The deglycosylation reaction was performed at 37 °C for 24 h in the presence/absence of Mn^{2+} (all in the absence of metal ion chelators) and visualized by SDS PAGE with GelCode Blue stain. Lower gel: N-glycanation in the presence of Mn^{2+}. HA was deglycosylated by PNGase F in the absence of metal ion chelators (50 nM Tris, pH 8.0) and then adjusted (treated) or not adjusted (control) to 1 mM $MnCl_2$. The control and treated reactions were then separated by SEC where the column and FPLC system were pre-equilibrated in 50 mM Tris, pH 8.0 ± $MnCl_2$. In both cases, a single peak corresponding to the HA trimer was collected and then visualized by SDS PAGE with GelCode Blue stain.

https://dx.doi.org/10.1021/acs.jproteome.9b00620
J. Proteome Res. 2020, 19, 733−743

which resolves the size difference between these two proteins (Figure 1B). SEC revealed that both input HA and the HA with reacquired CBD-PNGase F sensitivity had trimeric size (Figure 1B).

The above experiments were performed with recombinant HA that was coexpressed with neuraminidase to cleave terminal sialyl-oligosaccharide (SA) on HA. This prevents in-solution aggregation of HA trimers, as HA has lectin activity for SA.[22,25] To perform experiments in the presence of SA, we used Y98F HA, wherein this mutation attenuates binding to SA.[25] We found that the amidase-cleaved N-glycans also reappeared on Y98F HA when the amidase was removed from solution (Figure 1C).

Liquid Chromatography–Tandem Mass Spectrometry (LC–MS/MS) Reveals Cleavage and Reattachment of N-Linked Glycans

To test whether covalent *N*-glycan reattachment occurred during nondenaturing sample handling post PNGase F digestion and removal, we employed LC–MS/MS to profile tryptic digests of HA protein at each stage of the reaction (preamidase exposure, postamidase exposure, and postamidase removal; Figure 2, Figures S2–S9, and Table S1). As before, we ensured separation from CBD-PNGase F, using chitin affinity beads followed by SEC (Figure 1B). Over 90% of the amino acid sequence of HA was identified in the tryptic peptides, covering seven of the eight NXS/T sequons within HA (Figure S2). Prior to amidase treatment, N-linked glycan structures were detected at all seven of these sites (Figures 2B,C and S3–S9). The eighth sequon is near the N-terminus of the protein and was not detected at either the peptide or glycopeptide level. Glycan structures varied from simple inner core structures (e.g., GlcNAc2Man3 +/−Fuc) to higher-order sequences, including high mannose-type, hybrid-type, and complex biantennary structures (Figures 2B,C and S3–S9). We found that exposure to PNGase F under nondenaturing conditions efficiently removed the entire carbohydrate moiety at six of the seven measured NXS/T sites. Asn residue was identified as Asp by LC–MS/MS. However, for the peptide, NGLYPNLSK, deamidated Asn (Asp) was not observed in the presence of PNGase F, suggesting that glycans were not efficiently cleaved from this peptide by the amidase (Figure S9). Based on this observation, we inferred the absence of glycans on this peptide. It was not until we performed an in-depth search against the 38 common N-linked glycan library that we confirmed that this peptide was indeed glycosylated but not effectively de-N-glycosylated by PNGase F. However, glycans reappeared on the de-N-glycosylated peptides of the other six peptides bearing the NXS/T sequons, with compositions indistinguishable by MS (Figures 2B,C and S4–S9). These findings, along with the ability to repeatedly de-N-glycosylate the N-glycanated species using PNGase F, indicated that reattachment occurred at the same Asn residue. The HA was purified following coexpression with neuraminidase to prevent in-solution aggregation of the HA trimer,[22,25] and as a result, only trace levels of terminal SA were detected.

HA Forms a Noncovalent Complex with PNGase F Liberated Glycan, Prior to N-Glycanation

Our LC–MS/MS analyses indicated that glycans reattached to the same de-N-glycosylated peptides during N-glycanation, and the glycan structures observed after reattachment were indistinguishable by mass spectrometry from those observed prior to initial release (Figure 2B–D). We surmised that this could not occur if amidase-liberated glycan diffused freely away from the de-N-glycosylated HA. To evaluate this, we treated HA with PNGase F and then performed side-by-side SDS versus native PAGE following de-N-glycosylation. As previously observed, HA underwent de-N-glycosylation, as marked by the marked decrease in PAS staining in the SDS PAGE readout, indicating loss of carbohydrate (Figure 3A). However, when the same preparation was separated by native PAGE, PAS staining was not diminished, although a small downward shift in apparent MW was observed. These data suggested that the loss of glycan signal was SDS-dependent and that the glycans cleaved from HA remained noncovalently associated with HA in the presence of PNGase F.

To further test for complex formation, we separated the HA-PNGase F reaction by SEC immediately, without the prior use of magnetic beads for in-solution removal of the amidase. HA underwent concomitant N-glycanation during this chromatography: trimeric HA emerged, displaying a reacquired SDS-resistant glycan signal and reacquired sensitivity to PNGase F (Figure 3B,C). If HA was heat-inactivated (100 °C for 30 min) to provide amidase with denatured substrate, then *N*-glycan was no longer retained by HA, as indicated by PAS staining in the native PAGE readout (Figure 4A). Moreover, the denatured HA failed to undergo N-glycanation, as evaluated by de-N-glycosylation followed by separation of the HA-PNGase F reaction by SEC (Figure 4B). This suggested conformational control over the retention and reattachment of *N*-glycan at the deaminated NXS/T sequons. To further explore this, we mixed HA trimer with heat-denatured HA and then N-de-glycosylated the protein mixture together. The reaction components were then immediately separated by SEC, wherein the heat-denatured versus trimeric forms of HA could also be resolved by the size exclusion column used (Figure 4C). We found that only the native HA underwent N-glycanation during the chromatography and the denatured HA remained de-N-glycosylated (Figure 4C). This occurred despite the steric accessibility of NXS/T sequons in both forms of HA (as evaluated by the starting sensitivity of both trimeric HA and heat-inactivated HA to PNGase F; Figure 4B,C).

N-Glycanation in the Presence of Mn^{2+}

To control for enzymatic/PNGase F contribution to N-glycanation, we also performed the reaction in the presence of 1 mM Mn^{2+} which has been reported to inhibit the catalytic activity of this amidase.[29] We both confirmed Mn^{2+} as an inhibitor of PNGase F activity and also found that N-glycanation was not inhibited by 1 mM Mn^{2+} (Figure 4D).

N-Glycanation by Other Viral Glycoproteins/Vaccine Antigens

We found that N-glycanation also occurred for H3 and H5 trimers, which bear highly divergent amino acid sequences but not structures[32] (Figure S10). N-glycanation was also observed for the unrelated HIV Env but not for fetal bovine fetuin, a well-described glycoprotein substrate "standard" for PNGase F[12] (Figure S10). To confirm this difference, we performed the deglycosylation/N-glycanation procedure on a mixture of fetuin and HA. We found that within this mixture, only the latter underwent N-glycanation following removal of PNGase F (Figure S10), suggesting that fetuin may lack the protein conformational features needed to support this reaction.

https://dx.doi.org/10.1021/acs.jproteome.9b00620
J. Proteome Res. 2020, 19, 733–743

DISCUSSION

Protein N-glycans, including those of HA, have traditionally been analyzed following de-N-glycosylation by N-glycanases under denaturing conditions.[11−14,31] However, we found that following de-N-glycosylation under nondenaturing conditions, influenza HA spontaneously reversed this action and reformed the N-linkage when the N-glycanase was removed from solution. Reattachment to the Asp at de-N-glycosylated NXS/T positions was inferred by the repeated susceptibility to de-N-glycosylation by PNGase F (and the known consensus site required by deglycosidases), and our LC−MS/MS analysis indicating that glycans reattached to the same sequon-bearing peptide fragments of HA. Importantly, this was a nonenzymatic activity as N-glycanation also occurred in the presence of metal ions that inhibit catalysis by PNGase F.[29] Rather, glycan reattachment was preceded by noncovalent association of the cleaved glycans, and both steps required a folded protein substrate to proceed. Protein folding has long been predicted to support N-glycosylation within cells.[3,8,10,33,34] This new reaction, we term N-glycanation, suggests that under certain experimental conditions, some glycoproteins are capable of self-organizing the addition of their own glycans.

Spontaneous glycation of protein can proceed through the Maillard reaction in which a reducing sugar can react with the primary amino group provided by Lys.[35,36] However, this process normally happens slowly, requiring high temperature to accelerate. By contrast, we observed rapid reformation of PNGase F substrate at room temperature, where the magnetic bead separation was performed in less than 2 h, and for N-glycanation using SEC only, the separation between PNGase F and HA occurred within the first 20 min of the chromatography. Moreover, de-N-glycosylation followed by reformation of amidase substrate could be cycled repeatedly through iterative rounds of amidase exposure and removal, suggesting a two-state system in which N-linked glycan linkages were broken and then reformed. Normally, PNGase F catalyzes the hydrolysis of the amide bond of β-aspartylglycosylamine, liberating glycosylamine.[11−14] This reaction can also undergo reverse hydrolysis, a well-established principle where glycoside reactions are reversed so that the glycosidases, including N-glycanases, now catalyze synthesis (Asp back to Asn−glycan).[37−39] However, we observed the reformation of GlcNAc−β-Asn linkages from the deaminated positions when the N-glycanase was removed from solution, suggesting a different, glycosidase-independent, mechanism driving glycan reattachment.

Importantly, we found that N-glycanation was preceded by and also required the noncovalent retention of amidase-liberated glycans. This retention occurred in the presence of PNGase F and was disrupted by the addition of SDS. Free diffusing *N*-glycan would be unlikely to support a spontaneous reattachment process, and consequently, we hypothesized that intramolecular complexing near or at the de-N-glycosylated sequon could greatly lower the activation barrier to reattachment, potentially through reverse hydrolysis. We further hypothesized that if this noncovalent assembly was meaningful for N-glycanation, then the amidase-cleaved glycan should not separate from de-N-glycosylated HA if the PNGase F + HA mixture were immediately separated by SEC (i.e., no pre-in-solution depletion of PNGase F using magnetic beads). In support of these hypotheses, we found that cleaved *N*-glycan could not be separated from HA after exposure to PNGase F—rather, N-glycanation occurred during the chromatographic separation from PNGase F. These data suggested that noncovalent association between de-N-glycosylated HA and released glycans was a precursor step for N-glycanation, which is likely a simple chemical process. The fact that denatured HA was unable to both retain glycan in the presence of PNGase F and then undergo N-glycanation supports this conclusion and suggests that there was conformational control over glycan retention, aided by specific surface features that bind/trap carbohydrate. The observed differential capacity of glycoproteins to perform N-glycanation (HA vs HIV Env vs fetuin) may reflect differences in this conformational requirement.

While the chemical details of N-glycanation remain undefined, this reaction identifies a remarkable macromolecular-self-organizing capability wherein a complex glycan array, normally generated by the multiplexed activity of cellular biosynthetic enzymes, can be deconstructed and then reconstructed in simple test tube reactions, in the absence of cellular energy. This self-organizing activity also suggests potential utility in re-engineering some protein glycan sequences in vitro, a long-sought goal for glycoprotein therapies,[40,41] including within influenza and HIV vaccine development, where differential glycosylation of HA (the principal antigen for the seasonal flu vaccine) and also HIV Env can markedly affect bioactivity and vaccine efficacy.[17−21]

ASSOCIATED CONTENT

Supporting Information

The Supporting Information is available free of charge at https://pubs.acs.org/doi/10.1021/acs.jproteome.9b00620.

Table S1: list of common N-glycans; Figure S1: glycopeptide analysis workflow; Figure S2: spectral coverage of HA; Figure S3: MS glycoforms of Asn497 during N-glycanation; Figure S4: MS intensity heat map for glycopeptide CQTPQGAINSSLPFQNVHPVTIGECPK during N-glycanation; Figure S5: MS intensity heat map for glycopeptide NVTVTHSVNLLEDSHNGK during N-glycanation; Figure S6: MS intensity heat map for glycopeptide GIAPLQLGNCSVAGWILGNPECELLISK during N-glycanation; Figure S7: MS intensity heat map for glycopeptide ESSWPNHTVTGVSASCSHNGK during N-glycanation; Figure S8: MS heat map for glycopeptide ESWSYIVETPNPENGTCYPGYFADYEELR during N-glycanation; Figure S9: MS intensity heat map for glycopeptide NGLYPNLSK during N-glycanation; Figure S10: N-glycanation by other viral glycoproteins/vaccine antigens (PDF)

AUTHOR INFORMATION

Corresponding Authors

Steven A. Carr − *The Broad Institute of The Massachusetts Institute of Technology and Harvard University, Cambridge 02142, United States of America*; Email: scarr@broad.mit.edu

Daniel Lingwood − *The Ragon Institute of Massachusetts General Hospital, The Massachusetts Institute of Technology and Harvard University, Cambridge 02139, United States of America*; orcid.org/0000-0001-5631-9238; Email: dlingwood@mgh.harvard.edu

Authors

Celina L. Keating − *The Ragon Institute of Massachusetts General Hospital, The Massachusetts Institute of Technology and Harvard University, Cambridge 02139, United States of America*

https://dx.doi.org/10.1021/acs.jproteome.9b00620
J. Proteome Res. 2020, 19, 733−743

Eric Kuhn − *The Broad Institute of The Massachusetts Institute of Technology and Harvard University, Cambridge 02142, United States of America*
Julia Bals − *The Ragon Institute of Massachusetts General Hospital, The Massachusetts Institute of Technology and Harvard University, Cambridge 02139, United States of America*
Alexandra R. Cocco − *The Broad Institute of The Massachusetts Institute of Technology and Harvard University, Cambridge 02142, United States of America*
Ashraf S. Yousif − *The Ragon Institute of Massachusetts General Hospital, The Massachusetts Institute of Technology and Harvard University, Cambridge 02139, United States of America*
Colette Matysiak − *The Ragon Institute of Massachusetts General Hospital, The Massachusetts Institute of Technology and Harvard University, Cambridge 02139, United States of America*
Maya Sangesland − *The Ragon Institute of Massachusetts General Hospital, The Massachusetts Institute of Technology and Harvard University, Cambridge 02139, United States of America*
Larance Ronsard − *The Ragon Institute of Massachusetts General Hospital, The Massachusetts Institute of Technology and Harvard University, Cambridge 02139, United States of America*
Matthew Smoot − *The Ragon Institute of Massachusetts General Hospital, The Massachusetts Institute of Technology and Harvard University, Cambridge 02139, United States of America*
Thalia Bracamonte Moreno − *The Ragon Institute of Massachusetts General Hospital, The Massachusetts Institute of Technology and Harvard University, Cambridge 02139, United States of America*
Vintus Okonkwo − *The Ragon Institute of Massachusetts General Hospital, The Massachusetts Institute of Technology and Harvard University, Cambridge 02139, United States of America*
Ian Setliff − *Program in Chemical & Physical Biology, Vanderbilt University Medical Center, Nashville 37232-0301, United States of America; Vanderbilt Vaccine Center, Vanderbilt University, Nashville 37232-0417, United States of America*
Ivelin Georgiev − *Program in Chemical & Physical Biology and Department of Pathology, Microbiology, and Immunology, Vanderbilt University Medical Center, Nashville 37232-0301, United States of America; Vanderbilt Vaccine Center and Department of Electrical Engineering and Computer Science, Vanderbilt University, Nashville 37232-0417, United States of America*
Alejandro B. Balazs − *The Ragon Institute of Massachusetts General Hospital, The Massachusetts Institute of Technology and Harvard University, Cambridge 02139, United States of America*

Complete contact information is available at: https://pubs.acs.org/10.1021/acs.jproteome.9b00620

Author Contributions

[▽]C.L.K., E.K., J.B., A.R.C., and A.S.Y. contributed equally to this work.

Author Contributions

D.L. and S.A.C. designed the research studies; C.L.K, E.K., J.B., A.R.C., A.S.Y., C.M., M.S., L.R., M.S., T.B.-M., V.O., and I.S. performed the research; C.L.K, E.K., J.B., A.R.C., A.S.Y., I.G., A.B.B., S.A.C., and D.L. analyzed the data; and S.A.C. and D.L. wrote the paper.

Notes

The authors declare no competing financial interest.

■ ACKNOWLEDGMENTS

D.L. was supported by NIH grants (2P30AI060354-11, R01AI137057-01, DP2DA042422, and R01AI124378), the Harvard University Milton Award, The Gilead Research Scholars Program, and Strategic Initiatives from the Ragon Institute. This work was also made possible by an ENDHIV Catalytic Grant to D.L. and S.A.C. I.S. was supported by a Molecular Biophysics Training grant (T32 GM008320). The authors thank Dr. C.A. Lingwood (Hospital for Sick Children, Toronto) for helpful advice on these findings.

■ REFERENCES

(1) Schwarz, F.; Aebi, M. Mechanisms and principles of N-linked protein glycosylation. *Curr. Opin. Struct. Biol.* **2011**, *21*, 576−582.
(2) Moremen, K. W.; Tiemeyer, M.; Nairn, A. V. Vertebrate protein glycosylation: diversity, synthesis and function. *Nat. Rev. Mol. Cell Biol.* **2012**, *13*, 448−462.
(3) Mitra, N.; Sinha, S.; Ramya, T. N.; Surolia, A. N-linked oligosaccharides as outfitters for glycoprotein folding. form and function. *Trends Biochem. Sci.* **2006**, *31*, 156−163.
(4) Aebi, M. N-linked protein glycosylation in the ER. *Biochim. Biophys. Acta, Mol. Cell Res.* **2013**, *1833*, 2430−2437.
(5) Lu, H.; Fermaintt, C. S.; Cherepanova, N. A.; Gilmore, R.; Yan, N.; Lehrman, M. A. Mammalian STT3A/B oligosaccharyltransferases segregate N-glycosylation at the translocon from lipid-linked oligosaccharide hydrolysis. *Proc. Natl. Acad. Sci. USA* **2018**, *115*, 9557−9562.
(6) Chang, M. M.; Imperiali, B.; Eichler, J.; Guan, Z. N-Linked Glycans Are Assembled on Highly Reduced Dolichol Phosphate Carriers in the Hyperthermophilic Archaea Pyrococcus furiosus. *PLoS One* **2015**, *10*, No. e0130482.
(7) Taguchi, Y.; Fujinami, D.; Kohda, D. Comparative Analysis of Archaeal Lipid-linked Oligosaccharides That Serve as Oligosaccharide Donors for Asn Glycosylation. *J. Biol. Chem.* **2016**, *291*, 11042−11054.
(8) Shental-Bechor, D.; Levy, Y. Folding of glycoproteins: toward understanding the biophysics of the glycosylation code. *Curr. Opin. Struct. Biol.* **2009**, *19*, 524−533.
(9) Lu, D.; Yang, C.; Liu, Z. How hydrophobicity and the glycosylation site of glycans affect protein folding and stability: a molecular dynamics simulation. *J. Phys. Chem. B* **2012**, *116*, 390−400.
(10) Shental-Bechor, D.; Levy, Y. Effect of glycosylation on protein folding: a close look at thermodynamic stabilization. *Proc. Natl. Acad. Sci. USA* **2008**, *105*, 8256−8261.
(11) Lazar, I. M.; Deng, J.; Ikenishi, F.; Lazar, A. C. Exploring the glycoproteomics landscape with advanced MS technologies. *Electrophoresis* **2015**, *36*, 225−237.
(12) Morelle, W.; Faid, V.; Chirat, F.; Michalski, J. C. Analysis of N- and O-linked glycans from glycoproteins using MALDI-TOF mass spectrometry. *Methods Mol. Biol.* **2009**, *534*, 5−21.
(13) de Vries, R. P.; de Vries, E.; Bosch, B. J.; de Groot, R. J.; Rottier, P. J.; de Haan, C. A. The influenza A virus hemagglutinin glycosylation state affects receptor-binding specificity. *Virology* **2010**, *403*, 17−25.
(14) Cao, L.; Diedrich, J. K.; Kulp, D. W.; Pauthner, M.; He, L.; Park, S. R.; Sok, D.; Su, C. Y.; Delahunty, C. M.; Menis, S.; Andrabi, R.; Guenaga, J.; Georgeson, E.; Kubitz, M.; Adachi, Y.; Burton, D. R.; Schief, W. R.; Yates Iii, J. R.; Paulson, J. C. Global site-specific N-glycosylation analysis of HIV envelope glycoprotein. *Nat. Commun.* **2017**, *8*, No. 14954.
(15) Kwon, Y. D.; Finzi, A.; Wu, X.; Dogo-Isonagie, C.; Lee, L. K.; Moore, L. R.; Schmidt, S. D.; Stuckey, J.; Yang, Y.; Zhou, T.; Zhu, J.; Vicic, D. A.; Debnath, A. K.; Shapiro, L.; Bewley, C. A.; Mascola, J. R.; Sodroski, J. G.; Kwong, P. D. Unliganded HIV-1 gp120 core structures assume the CD4-bound conformation with regulation by quaternary interactions and variable loops. *Proc. Natl. Acad. Sci. USA* **2012**, *109*, 5663−5668.
(16) Zhou, T.; Lynch, R. M.; Chen, L.; Acharya, P.; Wu, X.; Doria-Rose, N. A.; Joyce, M. G.; Lingwood, D.; Soto, C.; Bailer, R. T.;

Ernandes, M. J.; Kong, R.; Longo, N. S.; Louder, M. K.; McKee, K.; O'Dell, S.; Schmidt, S. D.; Tran, L.; Yang, Z.; Druz, A.; Luongo, T. S.; Moquin, S.; Srivatsan, S.; Yang, Y.; Zhang, B.; Zheng, A.; Pancera, M.; Kirys, T.; Georgiev, I. S.; Gindin, T.; Peng, H. P.; Yang, A. S.; Program, N. C. S.; Mullikin, J. C.; Gray, M. D.; Stamatatos, L.; Burton, D. R.; Koff, W. C.; Cohen, M. S.; Haynes, B. F.; Casazza, J. P.; Connors, M.; Corti, D.; Lanzavecchia, A.; Sattentau, Q. J.; Weiss, R. A.; West, A. P., Jr.; Bjorkman, P. J.; Scheid, J. F.; Nussenzweig, M. C.; Shapiro, L.; Mascola, J. R.; Kwong, P. D.; et al. Structural Repertoire of HIV-1-Neutralizing Antibodies Targeting the CD4 Supersite in 14 Donors. *Cell* **2015**, *161*, 1280−1292.

(17) Hütter, J.; Rodig, J. V.; Hoper, D.; Seeberger, P. H.; Reichl, U.; Rapp, E.; Lepenies, B. Toward animal cell culture-based influenza vaccine design: viral hemagglutinin N-glycosylation markedly impacts immunogenicity. *J. Immunol.* **2013**, *190*, 220−230.

(18) de Vries, R. P.; Smit, C. H.; de Bruin, E.; Rigter, A.; de Vries, E.; Cornelissen, L. A.; Eggink, D.; Chung, N. P.; Moore, J. P.; Sanders, R. W.; Hokke, C. H.; Koopmans, M.; Rottier, P. J.; de Haan, C. A. Glycan-dependent immunogenicity of recombinant soluble trimeric hemagglutinin. *J. Virol.* **2012**, *86*, 11735−11744.

(19) Zhou, Q.; Qiu, H. The Mechanistic Impact of N-Glycosylation on Stability, Pharmacokinetics, and Immunogenicity of Therapeutic Proteins. *J. Pharm. Sci.* **2019**, *108*, 1366−1377.

(20) Bajic, G.; Maron, M. J.; Adachi, Y.; Onodera, T.; McCarthy, K. R.; McGee, C. E.; Sempowski, G. D.; Takahashi, Y.; Kelsoe, G.; Kuraoka, M.; Schmidt, A. G. Influenza Antigen Engineering Focuses Immune Responses to a Subdominant but Broadly Protective Viral Epitope. *Cell Host Microbe* **2019**, *25*, 827−835.

(21) Eggink, D.; Goff, P. H.; Palese, P. Guiding the immune response against influenza virus hemagglutinin toward the conserved stalk domain by hyperglycosylation of the globular head domain. *J. Virol.* **2014**, *88*, 699−704.

(22) Weaver, G. C.; Villar, R. F.; Kanekiyo, M.; Nabel, G. J.; Mascola, J. R.; Lingwood, D. In vitro reconstitution of B cell receptor-antigen interactions to evaluate potential vaccine candidates. *Nat. Protoc.* **2016**, *11*, 193−213.

(23) Whittle, J. R.; Wheatley, A. K.; Wu, L.; Lingwood, D.; Kanekiyo, M.; Ma, S. S.; Narpala, S. R.; Yassine, H. M.; Frank, G. M.; Yewdell, J. W.; Ledgerwood, J. E.; Wei, C. J.; McDermott, A. B.; Graham, B. S.; Koup, R. A.; Nabel, G. J. Flow cytometry reveals that H5N1 vaccination elicits cross-reactive stem-directed antibodies from multiple Ig heavy-chain lineages. *J. Virol.* **2014**, *88*, 4047−4057.

(24) Sangesland, M.; Kazer, S. W.; Ronsard, L.; Bals, J.; Boyoglu-Barnum, S.; Yousif, A. S.; Barnes, R.; Feldman, J.; Quirindongo-Crespo, M.; McTamney, P. M.; Rohrer, D.; Lonberg, N.; Chackerian, B.; Graham, B. S.; Kanekiyo, M.; Shalek, A. K.; Lingwood, D. Germline-encoded affinity for cognate antigen enables vaccine amplification of a human broadly neutralizing response against influenza virus. *Immunity* **2019**, *51*, 735−749.

(25) Villar, R. F.; Patel, J.; Weaver, G. C.; Kanekiyo, M.; Wheatley, A. K.; Yassine, H. M.; Costello, C. E.; Chandler, K. B.; McTamney, P. M.; Nabel, G. J.; McDermott, A. B.; Mascola, J. R.; Carr, S. A.; Lingwood, D. Reconstituted B cell receptor signaling reveals carbohydrate-dependent mode of activation. *Sci. Rep.* **2016**, *6*, No. 36298.

(26) Deng, X.; Zhang, J.; Liu, Y.; Chen, L.; Yu, C. TNF-alpha regulates the proteolytic degradation of ST6Gal-1 and endothelial cell-cell junctions through upregulating expression of BACE1. *Sci. Rep.* **2017**, *7*, No. 40256.

(27) Jones, M. B.; Oswald, D. M.; Joshi, S.; Whiteheart, S. W.; Orlando, R.; Cobb, B. A. B-cell-independent sialylation of IgG. *Proc. Natl. Acad. Sci. USA* **2016**, *113*, 7207−7212.

(28) Wittig, I.; Braun, H. P.; Schagger, H. Blue native PAGE. *Nat. Protoc.* **2006**, *1*, 418−428.

(29) Mussar, K. J.; Murray, G. J.; Martin, B. M.; Viswanatha, T. Peptide: N-glycosidase F: studies on the glycoprotein aminoglycan amidase from Flavobacterium meningosepticum. *J. Biochem. Biophys. Methods* **1989**, *20*, 53−68.

(30) Zhang, S.; Sherwood, R. W.; Yang, Y.; Fish, T.; Chen, W.; McCardle, J. A.; Jones, R. M.; Yusibov, V.; May, E. R.; Rose, J. K.; Thannhauser, T. W. Comparative characterization of the glycosylation profiles of an influenza hemagglutinin produced in plant and insect hosts. *Proteomics* **2012**, *12*, 1269−1288.

(31) Lazar, I. M.; Lee, W.; Lazar, A. C. Glycoproteomics on the rise: established methods, advanced techniques, sophisticated biological applications. *Electrophoresis* **2013**, *34*, 113−125.

(32) Paules, C.; Subbarao, K. Influenza. *Lancet* **2017**, *390*, 697−708.

(33) Xu, C.; Ng, D. T. Glycosylation-directed quality control of protein folding. *Nat. Rev. Mol. Cell Biol.* **2015**, *16*, 742−752.

(34) Helenius, A.; Aebi, M. Roles of N-linked glycans in the endoplasmic reticulum. *Annu. Rev. Biochem.* **2004**, *73*, 1019−1049.

(35) Zhang, Q.; Ames, J. M.; Smith, R. D.; Baynes, J. W.; Metz, T. O. A perspective on the Maillard reaction and the analysis of protein glycation by mass spectrometry: probing the pathogenesis of chronic disease. *J. Proteome Res.* **2009**, *8*, 754−769.

(36) Rabbani, N.; Ashour, A.; Thornalley, P. J. Mass spectrometric determination of early and advanced glycation in biology. *Glycoconjugate J.* **2016**, *33*, 553−568.

(37) Zeuner, B.; Jers, C.; Mikkelsen, J. D.; Meyer, A. S. Methods for improving enzymatic trans-glycosylation for synthesis of human milk oligosaccharide biomimetics. *J. Agric. Food Chem.* **2014**, *62*, 9615−9631.

(38) Lee, J. Y.; Park, T. H. Enzymatic in vitro glycosylation using peptide-N-glycosidase F. *Enzyme Microb. Technol.* **2002**, *30*, 716−720.

(39) Park, S. J.; Lee, J. Y.; Park, T. H. In Vitro Glycosylation of Peptide (RKDVY) and RNase A by PNGase F. *J. Microbiol. Biotechnol.* **2003**, *13*, 191−195.

(40) Gupta, S. K.; Shukla, P. Glycosylation control technologies for recombinant therapeutic proteins. *Appl. Microbiol. Biotechnol.* **2018**, *102*, 10457−10468.

(41) Lalonde, M. E.; Durocher, Y. Therapeutic glycoprotein production in mammalian cells. *J. Biotechnol.* **2017**, *251*, 128−140.

https://dx.doi.org/10.1021/acs.jproteome.9b00620
J. Proteome Res. 2020, 19, 733−743